SYNTHESIS OF ZINC OXIDE NANOPARTICLES USING *COLOCASIA ESCULENTA* LEAVES EXTRACT AND ANTIMICROBIAL STUDIES OF WHITE YAM PATHOGENS

Abstract

Zinc oxide nanoparticles (ZnO NPs) were synthesized by green method using aqueous leaves extract of *Colocasia esculenta*, L and characterized by UV-Visible, XRD, SEM, EDX and FTIR. The data obtained from the zone of inhibition (mm) was analyzed using statistical package for social science, SPSS Version 20. Results were reported as Mean ± SD. The statistical difference between more than 2 groups of data was evaluated using ANOVA with LSD post hoc test. Differences between means were considered significant at $p < 0.05$. The study revealed that maximum rate of synthesis could be achieved with 0.50 moldm^{-3} ZnO solution at 90 ^{o}C in 5 hours. Well segregated wurtzite hexagonal crystalline ZnO NPs with average crystallite size of 10 nm, ranging from 9.85 nm - 10.12 nm were obtained. FTIR spectra of the extract and the synthesized ZnO NPs revealed reducing agents such as phenolic groups as well as capping and stabilizing agents such as amines, peptides and amides groups. The biosynthesized ZnO NPs exhibited antimicrobial action in a dose-dependent manner against five white yam pathogenic fungi*: Aspergillus niger*, *Aspergillus flavus*, *Botryodioplodia theobromae*, *Phizopus stolenifera* and *Fusarium oxysporum* as well as three bacteria: *Klebsiella oxytoca*, *Serratia marcenscens* and *Pseudomonas aeruginosa.* The biosynthesized ZnO NPs exhibited effective to moderately effective inhibition ranging from 89.95 % to 32.22 % on the test organisms. The ZnO NPs favourably with standard antifungal *(*Ketoconazole*)* and antibacterial (Septrim) agents. The ZnO NPs holds great potential in reducing postharvest white yam tuber rot and many other related agricultural products losses as well as a source of active ingredients for antimicrobial drug formulation and development.

Key Words: Phytochemicals, nanotechnology, biosynthesis, pathogens, antimicrobial activity.

1.0 Introduction

One of the major challenges to food security in developing countries is the postharvest loss of agricultural products due to inadequate storage facilities, technological knowhow, and microbial-induced losses (Terngu, *et al*, 2024). Pathogens, especially fungi and bacteria have been identified as the major spoilage microbes of pre- and postharvest of crops because of their abilities to produce wide range of hydrolytic enzymes and mycotoxins (Desh, *et al*, 2014; Nath, *et al*, 2014). This has impacted negatively to food security, and safety.

Report has it that over 25 % of the yams produced in the world is lost annually to diseases and pests (FAO, 2011), and more than 50 % of the yam tubers produced and harvested in Nigeria is lost in storage (FAO,2023). Substantial losses occur during prolonged storage of yam; losses up to 10 – 20 % may occur during the first 3 months and 30 – 60 % after 6 months of storage (Gustavsson. *et al*, 2011 and Hodges *et al*., 2011). This has grave implication on food security, and sustainability with the attendant negative impact on national development.

Commented [user1]: The abstract should have a more defined structure, such as a clearer distinction between the **aim**, **methodology**, **results**, and **conclusion**. The current abstract mixes different elements in a way that can be hard for the reader to follow.

Deleted: .

Deleted: ,

Formatted: Font: Not Italic, Complex Script Font: Italic

Commented [user2]: It's important to summarize the key findings and conclusions in a manner that gives the reader a clear understanding of the significance of the research. This will make the abstract more impactful.

Commented [user3]: alphabetical order

Commented [user4]: The references in this section are very old, it is better to use the latest articles to get a proper track record.

Over the years, white yam tuber rots have been managed by conventional cultural control methods and use of synthetic chemicals like borax, captan, thiobendazole, benomyl and bleach (sodium hypochlorite) etc to inhibit the growth of pathogens during postharvest and postharvest stages (Gwa., *et al*, 2015; John *et al*., 2018). Although, the widely use of synthetic chemicals for white yam tuber rot control and prevention has been relatively effective because of their quick interventions and efficacies, there are limitations with some of the chemicals due to chemical residues, toxicity, pesticide resistance in target and non-target organisms (partly due to frequent and indiscriminate applications), non-biogradability, biomaccumulation, biomagnifications and biotransformations of the chemical residues along the food chain, thereby making them environmentally unfriendly. In addition, these chemicals are costly, not readily available, induce mutations, often discriminated against locally and internationally, and the lack of skills in the applications of these chemicals has adversely affected the environment (Gwa, *et al*, 2017). Antibiotic resistance is a major concern and development of new antimicrobial agents from plants in synergy with metal oxide could be useful in meeting the demand for new and effective antimicrobial agents with improved safety, biocompatibility and eco-friendliness). Other control measures involving gamma radiation (Imeh, and Jonah, 2012), and micro-organisms (Migrouna *et al*., 2003), also have their own limitations as farmers in developing countries such as Nigeria hardly adopt these measures because of cost implications and inadequate technological knowhow. The above sad narrative has great negative impact on food security and safety, sustainability, and national development.
Antimicrobial resistance is also a major concern and development of new antimicrobial agents from plants in synergy with metal oxide could be useful in meeting the demand for new and effective antimicrobial agents with improved safety, biocompatibility and eco-friendliness.

To address these concerns, there have been calls for eco-friendly natural products such as biosynthesized nanoparticles, which have been found to possess broad spectrum antimicrobial activities against pathogens of preharvest and postharvest white yam tubers as well as disease management in general. Nowadays, metal/metal oxides and plant extracts are used (either alone or in combination) at nonomeric scale (10^{-9}) as food preservatives. These are most effective for extending shelf life, stoppage or delay of microbial growth, suppressing the reactions when food comes in contact with oxygen or heat, enhancing food flavour and colours as well as preventing the loss of some essential nutrients (Gustavsson *et al*, 2011; Nwakoti, and Makurdi, 1989; Nigerian Stored Products Research Institute, 2006. Biological control is generally favoured as a method of disease management because it does not have the disadvantages of chemicals. Bioactive substances that are found bacterialstatic, bacterialcidal and/or fungicidal *in vitro* in most cases, kill the pathogens *in vivo* (Abubakar, and Osman, 1995; Okigbo, 2010; Okigbo, and Emeka, 2010*)*. The extract of plants offer little or no resistance from microorganisms, inhibit partially or completely microorganisms and are environmentally friendly (Dooshima et al, 2019). However, no single plant extract is capable of

inhibiting partially or completely all isolates that exist in associative growth in a system. Therefore, a composite mixture of plant extract in synergy with metal/metal oxide at nanomeric scale often gives a better result than that obtained from single plant extract (Rahayu *et al*, 2020).

The preliminary photochemical analysis of cocoyam leaves, stems, tubers and peels by many researchers revealed the presence of alkaloids, tannins, phenols, flavonoids, terpenoids, anthocyanins, steroids, saponins, glycosides and reducing sugars etc. in the extracts (Jane., *et al*, 1992; Richelle.*et al*, 2013; Eleazu, 2016). The corns also contain calcium oxalate, an irritant, which prevents them from being eaten raw or incompletely cooked (Eleazu, 2016). The presence of these photochemical confers antibacterial, antiviral, antifungal and antioxidant properties on cocoyam (Wang, 2012; Shinde, and Mengane, 2015; Pritha *et al*, 2015).

Zinc oxide (ZnO) on the other hand is a mineral ingredient of pharmacological preparations. It is known to have strong antimicrobial effects and is listed as Generally Recommend as Safe (GRAS) (Vassem., Umar, and Hahn, 2010; Yasser, and Nassium, 2019). ZnO is used to prepare formulations such as baby powder, barrier creams, antidandruff, shampoos, and antiseptic ointments to treat diaper dermatitis (diaper rash), protect the epidermis, prevent and treat sunburn (caused by ultraviolet rays), cuts, scapes, poisons ivy, and other skin conditions (Rahayu *et al*, 2020). ZnO has been used to fortify many products and its use as food additive is permitted (Yasser, and Nassium, 2019; Rahayu *et al*, 2020; Sunday, and Aderonke, 2020). Its toxicity and environmental profile in regards to human, animals and environment have been recommended by the United State Food and Drug Administration, US FDA (Rivero *et al*, 2021). The synergetic action of Zinc Oxide with cocoyam peel extracts at nanomeric scale has potentials to control postharvest white yam rot in Benue state. The cocoyam leaves mediated biosynthesized Zinc Oxide nanoparticles are easy to prepare and relatively reproducible, the active components are readily available and can be sourced locally. They are also affordable, non-phytotoxic and biodegradable, thus being friendly to man and the environment.

Commented [user5]: The connection between microbial spoilage and the need for eco-friendly solutions is clear, but the introduction could benefit from a stronger explanation of why *Colocasia esculenta* (cocoyam) was chosen specifically for this study. What makes its leaf extract particularly suitable for synthesizing ZnO nanoparticles compared to other plant materials?

Zinc oxide nanoparticles (ZnO NPs) have gained significant attention in recent years due to their unique properties and potential applications in various fields, including biomedical, cosmetics, electronics, photonics, catalysis, and environmental remediation, and agriculture among others (Zhang et al., 2018; Kumar et al., 2019). ZnO NPs possess unique properties, including antibacterial, photocatalytic, and UV-blocking abilities, making them ideal candidates for diverse applications (Sadeghi et al., 2019). They are widely used in products ranging from sunscreens and cosmetics to antimicrobial agents

This research focuses on the biosynthesis of zinc oxide nanoparticles (ZnO NPs) using cocoyam leaves extract and *In vitro* antimicrobial studies of the biosynthesized ZnO NPs against white yam tuber pathogens.

This study is intended to present a simple, affordable and readily available alternative method of yam tuber rot control and preservation to peasant farmers in Benue state, Nigeria to promote food security and sustainability for national development.

Commented [user6]: While the introduction references some studies on nanoparticles and antimicrobial activity, it could do more to link these references directly to the research gap. The introduction could be more explicit about the novelty of using *C. esculenta* leaf extract for biosynthesizing ZnO nanoparticles and the lack of research in this area, which this study aims to address.

2.0 Materials and Methods

2.1 Plants material and authentication

2.1.1 Collection of plant material

The *Colocasia esculenta* leaves were collected within the campus of the Benue State University, Makurdi in January, 2025. The leaves were properly labelled and packaged in clean cellophane bags.

Commented [user7]: It would be helpful to clarify whether only the leaves of *Colocasia esculenta* were used or whether other parts of the plant (such as stems or tubers) were also considered. Consistency in terminology and specificity about the plant parts used for extract preparation would reduce any potential confusion.

2.1.2 Identification and Authentication

The plant material was taken to the Department of Biological Sciences, Benue State University, Makurdi for identification and authentication before processing and analysis.

2.2 Drying and pulverization of the *Colocasia esculenta* leaves

The *Colocasia esculenta* leaves were thoroughly washed with distilled water and then dried under a shade at room temperature (to avoid chemical decomposition) for two weeks. Upon drying, the leaves were made into fine powder using a wooden mortar and pestle. The powder was kept in a plastic container with air tight lid.

2.2.2Plant extraction procedure

The extract was prepared by adding 100 g of powdered seeds to 500 mL of distilled water. The mixture was heated at 60 °C for 30 minutes, allowed to cool in a desiccator, and filtered to obtain the extract.

2.2.3 Storage of the extract

Stock solution (extract) was kept in the refrigerator at 4 ^{o}C for analysis.

2.3 Microorganism Handling

2.3.1 Source of microorganisms

Previously isolated and identified pathogens comprising of five fungi: *Aspergillus niger, Aspergillus flavus, Botryodioplodia theobromae, Rhizopus stolenifera*and *Fusarium oxysporum,* and three bacteria: *Klebsiella oxytoca, Serratia marcescens* and *Pseudomonas aeruginosa* were obtained from the Laboratory, Department of Biological Sciences, Benue State University, Makurdi where they were preserved and used for the antimicrobial study.

2.3.2 Culture media preparation

The methods of Clinical and Laboratory Standards Institute performance standards (CSLI) for antimicrobial discs tests, 2024; Terngu et al., 2024) were used with slight modifications. The cultured microorganisms were rehydrated in sterile distilled water and inoculated onto Potato Dextrose Agar (PDA) and Nutrient Agar (NA) for fungi and bacteria respectively. Following incubation at 37 ^{o}C for 24 hours, the cultures were sub-cultured on fresh PDA and NA for fungi and bacteria respectively. Stocks for long term storage was also prepared in 20 % glycerol and kept at 70 ^{o}C.

The cultures were maintained at 4 ^{o}C and sub-culturing was done regularly to maintain fresh cultures for the experiment. Before use, the purity of each culture was also confirmed by using culture identification guides. The grown colonies were the harvested and dispersed in PDA (fungi) and NA (bacteria), and the turbidity of the suspension was adjusted to an optical density of (OD_{550} nm) 0.144, which is equivalent to 1.0 x 10^{6} cells/mL.

All reagents used were analytical grade and used as received without further purification. All solutions were freshly prepared using double-distilled water and kept in the dark to avoid photochemical reactions. All glassware used in the experimental procedures were sterilized in 10 % sodium hypochlorite solution, rinsed thoroughly in double-distilled water and dried before use. Aseptic condition was maintained throughout the experiments.

2.3 Qualitative Phytochemical Analysis

Qualitative Phytochemical analysis of alkaloids, cardiac glycosides, flavonoids phenols, resins, saponins, tannins, terpenes and steroids were done using standard phytochemical methods (AOAC., 2023).

i. Tests for alkaloid

Preliminary test (Dragendorff reagent test)

A few drops of Dragendorff reagent were added to 2 mL of the extract and a solution of potassium bismuth iodine was also added and observed for orange colouration.

Confirmatory test (Wagner reagent test)

To 3 drops of the Wagner Reagent, 2 mL of the extract were added, followed by a solution of iodine in potassium iodine . The formation of deep brown precipitate would indicate the presence of alkaloid.

ii. Tests for cardiac glycoside

Preliminary test (Lieberman's test)

To 2 mL of the plant extract, 2 mL of acetic anhydride was added and cooled in ice. Sulphuric acid was added carefully along the side of the test tube. A colour change from violet to blue green indicates the presence of steroid nucleus (i.e. a glycone portion of the cardiac glycoside).

Confirmatory test (Salkowski test)

To 2 mL of the extract, 2 mL of chloroform were added to dissolve the extract. Sulphuric acid was then carefully added to form a lower layer. A reddish–brown colour at the interphase indicates the presence of cardiac glycoside.

iii. Test for flavonoids

A few drops 10 % of lead acetate solution was added to 2 mL of the extract in a test tube. The observation of either cream or light yellow colourations confirms the presence of flavonoids.

iv. Test for phenols

To 2 mL of the extract, 2 mL of ferric chloride was added. A deep blush green solution indicates the presence of phenols.

v. Test for resins

To 2 mL of acetic anhydride, 2 mL of the extract was added, followed by a drop of concentrated sulphuric acid was also added. The observation of a purple colour rapidly changing to violet indicates the presence of resins.

vi. Test for saponins

To 5 mL of distilled, 2 mL of the extract was added in a test tube. This was shaken vigorously after which a few drops of olive oil was added. Formation of an emulsion will indicate the presence of saponins. Also the formation of persistent foams during plant extraction or during the concentration of plant extract is reliable evidence that saponins are present.

vii. Tests for Tannins

Preliminary test

1 mL of the extract was diluted with 4.ml of distilled water (in a ration 1:4) and a few drops of 10 % very dilute ferric chloride solution was gradually added to the aqueous extract. The presence of blue or green precipitate or colourations shows the presence of tannins.

Confirmatory test

To 3 drops of lead acetate solution, 2 mL of the extract was added. The resulting solution was then observed for brown precipitate which indicated the presence of tannins.

viii. Test for Terpenes and Steroids

To 1 mL of acetic anhydride, 2 mL of the extract was added and then concentrated sulphuric acid was carefully added down the side of the test tube. An observation for reddish brown colour at the interphase indicates the presence of terpenes and steroids.

Commented [user8]: he methodology is thorough but could be better organized. For example, grouping the various phytochemical tests into categories (e.g., alkaloids, flavonoids, tannins, etc.) would improve **readability and coherence**.

2.4 Synthesis of Zinc Oxide Nanoparticles (znO NPs)

The method described by *Farjana* et al, (2022) was used with slight modification. 10 mL aqueous 0.50 $moldm^{-3}$ ZnO was mixed with 5 mL of the extract in a 250 mL beaker. Then, the pH of the solution was

adjusted to 12 by a drop-wise addition of 0.02 moldm-3aqueous solution of NaOH. The influence of temperature on ZnO NPs formation was studied by heating the solution on a water bath from 4 ºC - 80 ºC with constant stirring using a magnetic stirrer for 4 hours. The solution was cooled to 30 ºC, purified by centrifugation at 1200 rpm for 5 minutes to obtain white precipitates. The precipitates were then washed four times with deionized water, dried for 24 hours at 80 ºC and stored in a desiccator for further analysiss

Commented [user9]: The synthesis procedure is generally clear, but the section would benefit from more detail about the temperature conditions and the role of temperature in the formation of nanoparticles. Consider providing more information on why a 5-hour reaction time at 80°C was chosen and its significance in the nanoparticle synthesis process

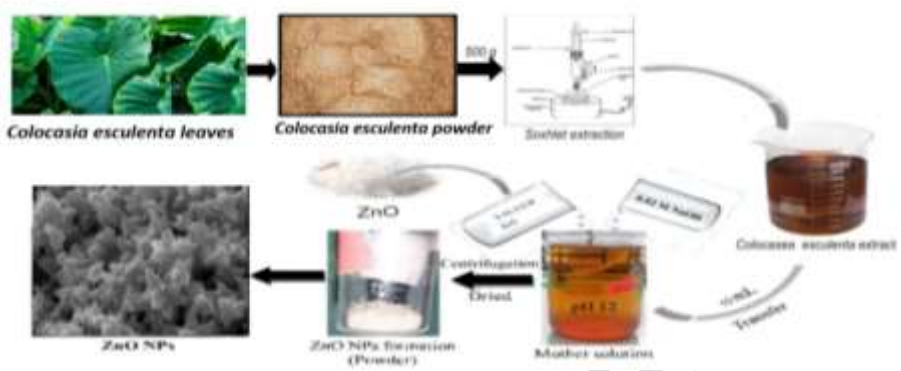

Fig. 1: A modified schematic diagram for the preparation of ZnO NPs using *C esculenta* leaves extract (Farjana *et al,* 2022).

2.5 Characterization of ZnO NPs

The biosynthesized ZnO NPs were characterized by UV-visible spectroscopy, X-Ray Diffraction (XRD) analysis, Scanning Electron Microscopy (SEM), Energy Dispersive X-ray (EDX) and Fourier Transform Infrared (FTIR) spectroscopy. Uv-Vissible spectrophotometer (Uv-3600 Plus, Shimadzu, Japan) in the range of 350-700 nm was used to confirm the formation of the ZnO NPs. Phase and unit cell dimension information was determined with the use of XRD-6000, Shimadzu, Japan with monochromatic Cu Ka radiation (1.5419 Å), operated at 40 kV and 30 mA at 2θ (25- 75º) and speed of 4º per minutes. SEM equipped with EDX (Philips XL-30, Eindhoven, Netherlands) was used to study the surface morphology and elemental composition of the ZnO NPs. FTIR analysis of the ZnO NPs was performed with Perkin Elmer FTIR Spectrophotometer-100 with the KBr pellet method in the range of 500 - 4000 cm^{-1} to determine the functional groups responsible for the reduction of the Zn^{2+} as well as capping and stabilizing agents of the ZnO NPs.

2.6 Antimicrobial Sensitivity Test

The methods of Shiriki *et al*., 2015; Terngu**.,** *et al*., 2024) were employed with slight modification. The biosynthesized ZnO NPs was tested against five previously isolated and identified white yam pathogenic fungi: *Aspergillus niger, Aspergilus flavus, Botryodioplodia theobromae, Phizopus stolenifera* and *Fusarium oxysporum* as well as three bacteria: *Klebsiella oxytoca, Serratia marcenscens,* and *Pseudomonas aeruginosa*. The pure isolates were individually cultured on ZnO NPs incorporated Potato Dextrose Agar (PDA) and Nutrient Agar (NA) plates for fungi and bacteria respectively and incubated at 37 ^{o}C for 7 days (fungi) and 24 hours (bacteria). Triplicates samples were prepared. The controls consisted of 1 mL 100 % Ketoconazole (200 mg) and 100 % of 1 mL Septrim (480 mg) tablets for fungi and bacteria respectively. Zone of inhibition (mm) where present was recorded with a transparent plastic ruler after the incubation period and the percentage inhibition zones calculated as follows:

% Inhibition Zone (% IZ) = Average diametre of pathogen colony / Average diametre of pathogen in control x 100% (5)

The percentage inhibition was rated on the scale described by Pritha *et a*l (2015; Terngu**.,** *et al*, 2024) as follows:

100 % inhibition (highly effective); 50 – 99 % inhibition (effective); 20 – 49 % inhibition (moderately effective); 0 – 19 % inhibition (slightly effective) and ≤ 0 % inhibition (not effective).

2.7 Statistical Analysis

The data obtained from the zone of inhibition (mm) was analyzed (descriptive statistics and inferential statistics to report the findings and to test hypothesis at 0.05 level of significance respectively) using statistical package for social science, SPSS Version 21. Results were reported as Mean ± SD. The statistical difference between more than 2 groups of data was evaluated using ANOVA with LSD post hoc test. Differences between means were considered significant at $p < 0.05$.

3. 0 RESULTS AND DISCUSSION

3.1 Phytochemical Screening

Table 1: Result of phytochemical screening

Secondary Metabolite	Test	Result
Tannins	$FeCl_3$ Test	+
Saponins	Froth test	+
Flavoniods	Lead Acetate Test	+
Phenols	Ferric Chloride Test	+
Alkaloid	Hager's Test	+
Steroids	Libbermann Burchard's Test	+
Quninones	Hydrochloric Acid Test	-
Starch	Iodine Test	+
Terpenoids	Sakocoski's Test	+

Glycosides	Keller-Kallani's Test	+

Table 1 presents the result of the phytochemical analysis of *C. esculenta* tuber leaves extract. The result indicated the presence of tannins, saponins, flavonoids, phenolics, alkaloids, steroids, starch, terpenoids and glycosides.

3.2 UV-Visible Spectroscopy Analysis

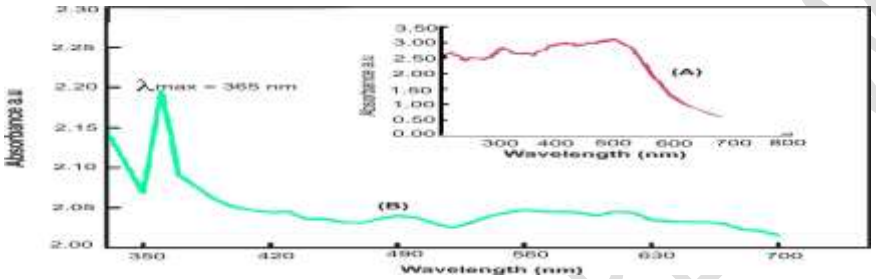

Fig. 2. UV-Vis spectra of (A) *Colocasia esculenta* leaves extract and (B) the biosynthesized ZnO NPs recorded as a function of reaction time.

UV-visible spectroscopic analysis was conducted to monitor the progress of the biogenic formation of ZnO NPs. The interaction between Zn^{2+} containing solution (Zn acetate) and the *C. esculenta* leaves extract shows λmax at 370 nm with the absorption steadily building up with time and increasing temperature, reaching a maximum at 80 ^{0}C in 4 hours with a colour change from light orange to white, indicating the formation of ZnO NPs. Similarly, the Uv-visible analysis of the extract showed many peaks at different wavelengths, ranging from 210 nm to 530 nm. The presence of the phytochemicals in the extract was responsible for the reduction of the zinc ions (Zn^{2+}), stabilization, and capping of the ZnO NPs.

3.3 X-Ray Diffraction Analysis

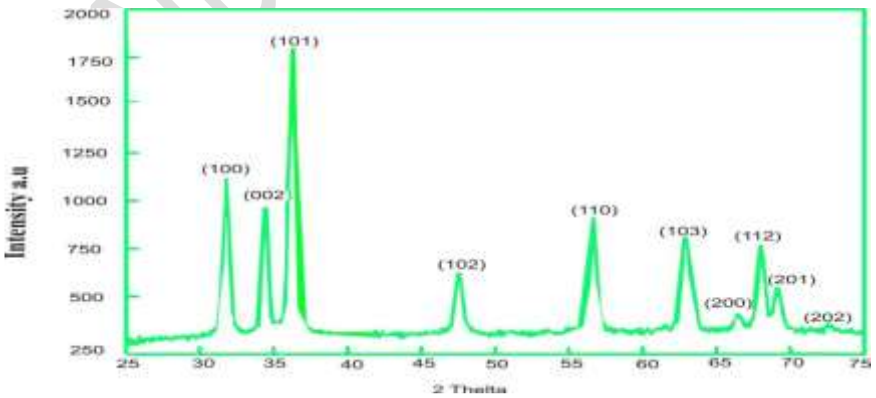

Fig. 3: XRD pattern of the biosynthesized ZnO NPs

Fig. 3 represents the XRD spectra of the ZnO NPs. The XRD spectra revealed ten distinctive diffraction peaks at 2θ angles of 31.84^0, 34.50^0, 36.260, 47.57^0, 56.56^0, 62.90^0, 66.42^0, 67.92^0, 69.190 and 77.02^0. Diffraction peaks are converted to d-spacing which is characteristic for each material that allow for the identification of the material. The diffracted peaks above can be assigned to miller indices of 100, 002, 101, 102, 110, 103, 200, 112, 201 and 202 respectively, corresponding to the reflection lines of hexagonal wurtzite structure according to the Joint Committee on Powder Diffraction Standards (JCPDS) card no: 36-1451 (Ramesh, *et al*., 2014;; Terngu**.,** *et al*, 2024).

The average crystallite size of the ZnO NPs was estimated by the Debye-Scherrer`s equation

$d = k\lambda/\beta\cos\theta$ (Khariossova., et al, 2013; Terngu**.,** *et al*, 2024) where d = crystallite size (nm), k = correction/shape factor (0.9), β = full width at half maximum (FWHM) and θ = Bragg`s angle (rad). The average crystallite size of the biosynthesized ZnO NPs was calculated to be 10 nm with the range 10.12 nm – 9.85.

3.4 Scanning Electron Microscopy (SEM) With Energy Dispersive X-Ray (EDX)

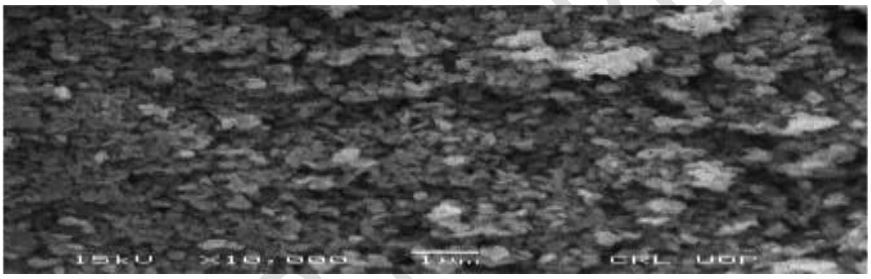

Fig. 4: SEM image of biosynthesized ZnO NPs

Commented [user10]: The SEM image is mentioned but not fully described in the text. It would be helpful to explain the significance of the observed "hexagonal shapes" in the context of ZnO nanoparticle formation. Additionally, the discussion could benefit from clarifying why the morphology and crystallinity of these nanoparticles are important for their antimicrobial activity.

The size and surface morphology as well as elemental composition of the biosynthesized ZnO NPs was analyzed using SEM hyphenated energy dispersive X-ray (EDX). The SEM image of the ZnO is presented in Fig. 4.

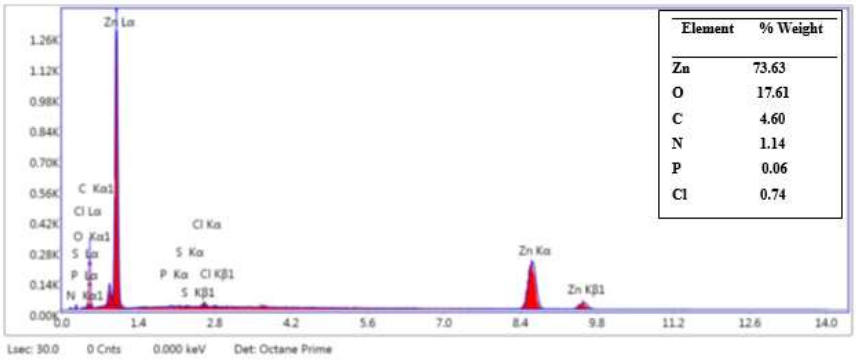

Element	% Weight
Zn	73.63
O	17.61
C	4.60
N	1.14
P	0.06
Cl	0.74

Fig. 5: EDX spectrum of the biosynthesized ZnO.

Commented [user11]: The EDX spectrum shows the elemental composition, but more discussion on the significance of the detected elements (e.g., Zn and O) in the context of nanoparticle purity and effectiveness would be useful

The calculation of the crystallite size of the ZnO NPs using ImageJ software gives the size of about 10.99 nm, which is in agreement with the calculated crystallite size of 11.00 nm from XRD data using the Debye-Scherrer equation. The SEM images (Figure 4) revealed segregated hexagonal shapes with good crystallinity.

Fig. 5 shows the chemical composition of the ZnO NPs with their respective percentages. The EDX spectrum shows characteristic peaks and elemental composition of Zn and Oxygen (73.63%) and O (17.61%) respectively, but low percentage of C, N, P, S and Cl which indicate high purity of the biosynthesized ZnO NPs.

3.5 Fourier Transform Infra-Red Spectroscopy (FTIR) Analysis

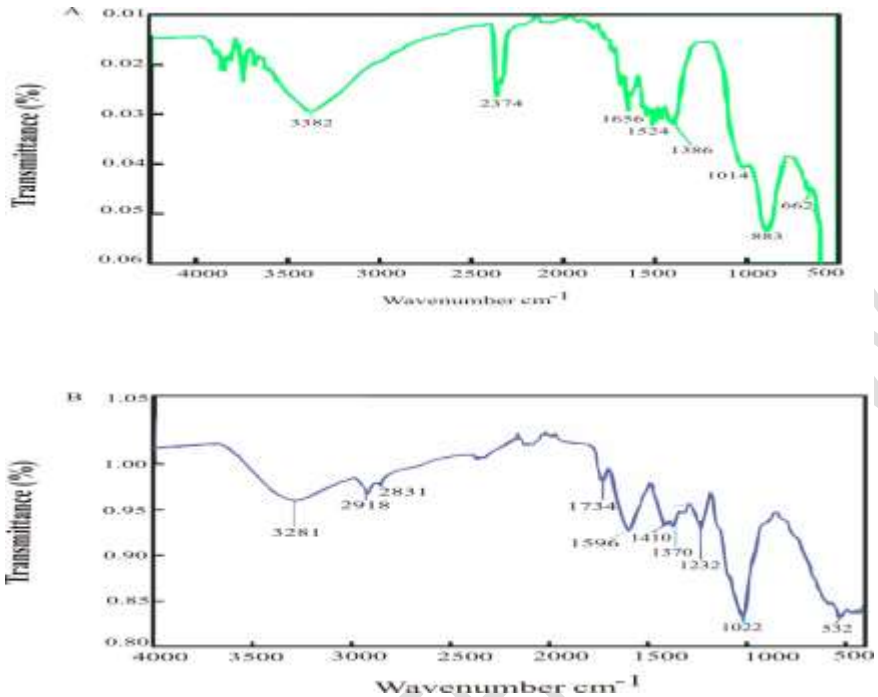

Figure 6: FTIR spectra of (A) the biosynthesized ZnO NPs and (B) *Coocasia. Esculenta* leaves extract.

The small peak at 662 cm^{-1} in the FTIR spectrum of the ZnO NPs is allotted to the hexagonal wurtzite phase Zn-O stretching vibration. The broad peak at 3382 cm^{-1} is characteristic of stretching vibration of hydroxyl group (O-H) from polyphonols. The peak at 2374 cm^{-1} is attributed to the H-O-H vibrations of water molecules of crystallization. The peaks at 1656 cm^{-1}, 1524 cm^{-1}, 1380 cm^{-1}, 1014 $cm^{-1}$and 883 cm^{-1} are assigned to bending vibrations of C=C stretching of alkene, aromatic ring and polyphenols (C=O),
C-H bending vibrations of alkane groups, stretching of C≡N, and bending vibrations of C-H respectively.
The FTIR analysis of the *C. esculenta* leaves extract shows peaks at 3281 cm^{-1} which represents the symmetric O-H stretching, while that at 2918 cm^{-1} is assigned to phospholipids cholesterol and creatine. The peak at 2831 cm^{-1} and 1734 cm^{-1} correspond to the C-H and C=O stretching respectively, while that at 1596 cm^{-1} represents C≡N and NH_2 respectively. The peak at 1410 cm^{-1} is assigned to stretching C≡N, N-H and C-H deformations. Peaks 1370 cm^{-1} corresponds to N-H deformation, while the peak at 1232 cm^{-1} is allocated to the overlapping of the protein amide III and the nucleic acid phosphate vibrations. The peaks at 1022 cm^{-1} and 532 cm^{-1} are assigned to the glycogen and sulphur compounds respectively.
The FTIR analysis confirmed the presence of functional groups from phytochemicals such as tannins, saponnins, alkaloids, terpenes, flavonoids, phenols, steroids, and aromatic hydrocarbon, amines, amides etc

which are responsible for the reduction of the Zn ions as well as capping and stabilizing agents of the ZnO NPs.

Table 2: Average zone of inhibition (mm) of the biosynthesized ZnO NPs

	Zinc Oxide Nanoparticles Concentration (mg/mL)				
	100	**75**	**50**	**25**	**Control**
Fungi					
Aspergillus niger	6.91 ± 0.08^{c}	6.83 ± 0.42^{c}	5.83 ± 0.42^{b}	3.67 ± 0.52^{a}	8.16 ± 0.41^{d}
Aspergillus flavus	7.98 ± 0.04^{c}	7.50 ± 0.54^{c}	6.33 ± 0.51^{b}	5.20 ± 0.20^{a}	9.67 ± 0.52^{d}
Botryodioplodia theobromae	8.16 ± 0.42^{c}	7.50 ± 0.54^{b}	7.00 ± 0.63^{b}	6.67 ± 0.32^{a}	11.00 ± 0.89^{d}
Rhizopus stolenifera	13.67 ± 0.52^{d}	8.16 ± 0.98^{c}	7.50 ± 0.55^{b}	5.80 ± 0.41^{a}	18.00 ± 0.63^{e}
Fusarium oxysporum	25.50 ± 0.55^{d}	20.33 ± 0.52^{c}	17.33 ± 0.52^{b}	12.33 ± 0.52^{a}	29.67 ± 0.52^{e}
Bacteria					
Klebsiella oxytoca	26.00 ± 0.89^{d}	20.33 ± 0.52^{c}	18.33 ± 0.52^{b}	15.67 ± 0.52^{a}	34.83 ± 0.75^{e}
Serratia marcescens	34.67 ± 0.82^{d}	26.00 ± 0.89^{c}	22.33 ± 0.52^{b}	18.33 ± 0.42^{a}	40.33 ± 0.52^{e}
Pseudomonas aeruginosa	35.16 ± 0.42^{d}	30.83 ± 0.98^{c}	25.33 ± 0.52^{b}	18.33 ± 0.52^{a}	37.67 ± 0.52^{e}

N= 5, values expressed as Mean ± SD. Values in the same row with different alphabetical letters (superscript) are statistically significant at $p < 0.05$.

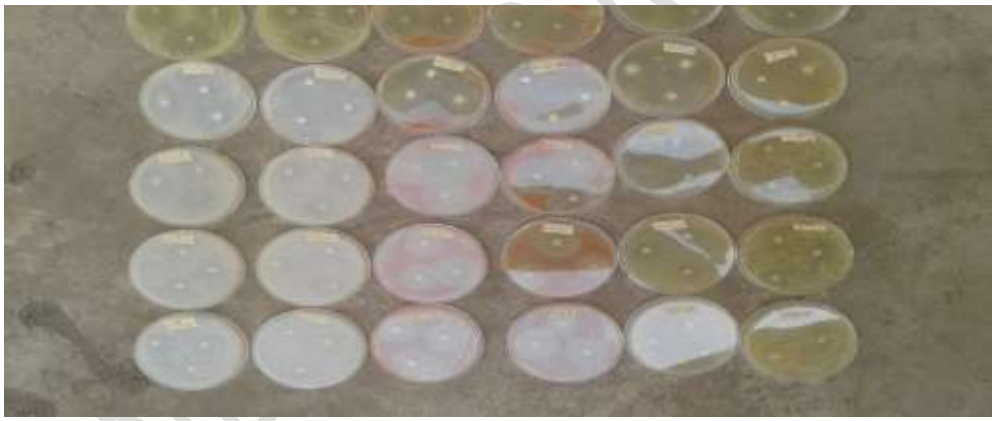

Figure 7: Antimicrobial sensitivity test plates.

Table 3: Percentage zone of inhibition of the ZnO NPs

Concentration (mg/mL)	100	75	50	25
Fungi				
Aspergillus niger	84.68	83.70	71.45	44.98
Aspergillus flavus	82.52	77.56	65.46	53.77
Botryodioplodia theobromae	74.18	68.18	63.64	60.64
Rhizopus stolenifera	75.94	45.33	41.67	32.22
Fusarium oxysporum	85.95	68.52	58.41	41.56

Bacteria				
Klebsiella oxytoca	75.94	45.33	41.67	32.22
Serratia marcescens	85.95	68.52	58.41	41.56
Pseudomonas aeruginosa	74.65	58.37	52.63	44.99

Key:
a = 100 % inhibition (highly effective)
b = 50 – 99 % inhibition (effective)
c = 20 – 49 % inhibition (moderately effective)
d = 0 -19 % inhibition (slightly effective)
e = ≤ 0 % inhibition (not effective) (Sangoyomi, 2004; Terngu**.,** et al, 2024).

For table 2 and 3:

These tables present detailed results, but some of the data analysis could be more thorough. For instance, the interpretation of the statistical significance and the comparison with standard antibiotics could be better explained. A brief summary of the statistical significance of the differences observed would be beneficial to the reader.

3.6 Antimicrobial Study of the ZnO Nanoparticles

The antimicrobial study of the ZnO NPs was carried out against five previously isolated and identified white yam pathogenic fungi: *Aspergillus niger*, *Aspergillus flavus*, *Botryodioplodia theobromae*, *Rhizopus stolenifera* and *Fusarium oxysporum*, and three bacteria: *Klebsiella oxytoca*, *Serratia marcenscens*, and *Pseudomonas aeruginosa*. Table 2 represents the average zone of inhibition (mm), while Table 3 shows the percentage zone of inhibition (% IZ) of ZnO against the isolates.

Generally, the results showed that the inhibitory effects of the biosynthesized ZnO NPs increased with increasing concentration ($p < 0.05$). The result revealed average zone of inhibition (mm) that is significant at $p < 0.05$. The biosynthesized ZnO NPs showed effective to moderately effective inhibition against all the test organisms at 100 mg/mL; effective inhibitions against *Aspergillus niger*, *Aspergillus flavus Botryodioplodia theobromae*, *Fusarium oxysporum*, *Serratia marcenscens*, and *Pseudomonas aeruginosa* at 75 mg/mL and 50 mg/mL respectively while *Rhizopus stolenifera* and *Klebesiella oxytoca* recorded moderately effective inhibition at the same concentrations. *Botryodioplodia theobromae* and *Aspergillus flavus* were effectively inhibited 25 mg/mL, while *Aspergillus niger*, *Fusarium oxysporum*, *Rhizopus stolenifera*, *Klebesiella oxytoca*, *Serratia marcenscens*, and *Pseudomonas aeruginosa* recorded moderately effective inhibition at the same concentration. The results are effective against the test microorganisms when compared with standard antimicrobial agents: Ketoconazole and septrim ($p < 0.05$).

Commented [user12]: The antimicrobial results are promising, but the discussion could be enriched by explaining why ZnO nanoparticles were effective against certain pathogens and not others. Are there any specific properties of the pathogens or the nanoparticles that could explain these differences? Further, a comparison of your findings with those of similar studies in the literature would strengthen the discussion.

4.0 Conclusion

ZnO NPs was effectively synthesized through the green route approach using *C. esculenta* leaves extract. Characterization of the biosynthesized ZnO NP showed hexagonal wurtzite crystal structure with an average crystallite size of 10.99 nm, ranging from 10.12 nm to 9.85 nm formed at 365 nm by UV-Vis analysis. SEM and EDX analyses showed clearly segregated hexagonal ZnO NPs with higher percentage weights of Zn

and O, but lower percentages of C, N, P, S, and Cl, suggesting high purity. The ZnO NPs' reduction, capping, and stabilization were all caused by organic functional groups, which the FTIR analysis verified were present.

The antimicrobial study of the ZnO NPs against white yam pathogens compared favourably with standard antifungal (ketoconazole) and antibacterial (Septrim) agents. *In vitro* antimicrobial analysis of the biosynthesized ZnO NPs showed great potential in controlling and/or preventing white yam tuber rot and can provide an alternative to synthetic antimicrobial agents since it is less expensive, environmentally friendly, biocompatible and easy to prepare. The ZnO NPs will serve as an active ingredient in antimicrobial drug formulation and development as well as contribute greatly in improving food security and safety.

References

Ahmed, S.A., Taia, A., Ahmad, O.B., Samy, S., Abir, M.H. (2022). A.Green Synthesis and Characterization of ZnO Nanoparticles Using *Pelargonium odoratissimum*(L.) Aqueous Leaf Extract and Their Antioxidant, Antibacterial and Anti-inflammatory Activities. *Antioxidants (Basel).*2022;(8):1444.DOI:10.3390/antiox11081444.Available:https://doi.org/10.4236/fns.2017. 87051.

Amin, G., Asif, M.H., Zainelabidin, A., Zaman, S., Nur, O., Willander, M. (2011). Influence of Ph, precursor concentration, growth time, and temperature on the morphology of Zno nanostructures grown by the hydrothermal method. *Journal of Nanomaterials.* 2011;269692.

Divya, M.J., Sowmia, C., Joona, K., Dhanya, K.P. (2013). Synthesis of zinc oxide nanoparticle from Hibiscus rosa-sinensis leaf extract and investigation of its antimicrobial activity. Res; 2013.

Eleazu, C.0. (2016). Characterization of the natural products in cocoyam (*Colocasia esculenta)* using GC-MS. *Pharmaceutical Biology*. 2016;54(12):2880-2885.

Elumalai, K., Velmurugan, S. (2015). Green synthesis, characterization and antimicrobial activities of zinc oxide nanoparticles from the leaf extract of *Azadirachta indica* (L). *Applied Surface Science*. 2015;345**:**329-36.

Jha, A.K., Kumar, V., Prasad, K. (2011). Biosynthesis of metal and oxide nanoparticles using orange juice. J. Bionanoscience. 2011;5(2):162–166. Available:http://dx.doi.org/10.1166/jbns.2011.1053.

Farjana, R., Md Abdul M.P., Md Abu, B.S, Muhammad, S.B, Md. Aminul, H., Beauty, A., Rimi, R., Md. Anamul, H., Royhan, A.K.M. (2022). Green synthesis of ZnO nanoparticles using Cocos nucifera leaf extract: Characterization, antimicrobial, antioxidant, and photocatalytic activity; 2022. Available:https//doi.org/10.11012020.10.27.514023.

Jayanta, K. B. (2013). Synthesis and characteriztion of zno nanoparticles. a master of science dissertation of the department of physics. National Institute of Technology, Rourkela, Orissa, India; 2020.

Josef, J., Katarina, K. (2015). Application of nanotechnology in agriculture and food industry, its prospects and risks .*Ecol chem Eng* s. 2015;22(3):321-361.

Kharissova, O.V., Dias, H.V.R., Kharisov, B.I, Perez, B.O, Perez, V.M.J. (201). The greener synthesis of nanoparticles *Trends in Biotechnology*. 2013;31(4):240-48.

Kumar et al. (2019). Zinc oxide nanoparticles: A review of their antimicrobial activity and applications in medicine. *Journal of Nanoparticle Research*, 21(10).

Lakshmi, J.V., Sharath, R., Chandraprabha, M.N., Neelufar, E., Hazra, Abhishikta, Patra, Malyasree Synthesis, characterization and evaluation of antimicrobial activity of zincoxide nanoparticles. *J. Biochem. Technology*. 2012;3(5):S151–S154.

Mittal, A.K., Chisti, Y., Banerjee. U.C. (2013). Synthesis of metallic nanoparticles using plant extracts *Biotechnol Adv*; 2013. DOI: 10.1016/*j.biotechadv*.2013.01.003.

Moloto, N., Revaprasadu, N., Musetha, P.L, Moloto, M.J. (2009). The effect of precursor concentration, temperature and capping group on the morphology of CdS nanoparticles. *Journal of Nanoscience and Nanotechnology*. 2009;9:4760-66.

Nakade, D.B., Mahseh, S.K., Kiran, N.P., Vinayak, S.M. (2013) Phytochemical screening and Antibacterial Activity of Western Region wild leaf *Colocasea esculenta*. *International Research Journal of Biological Science*. 2013;2(10):1-6.

Official Methods of Analysis of AOAC International. (2023). 22nd ed. AOAC International, Gathersburg, MD, USA, Official Methods, 2023.005.

Padil, V.V.T, Cernik, M. (2013). Green synthesis of copper oxide nanoparticles using gum karaya as biotemplate and their antibacterial application. *International Journal of Nanomedicine. 2013;8:889-98.*

Parveen, K., Banse, V., Ledwani, L (2015). Green synthesis of nanoparticles: Their advantages and disadvantages 2nd International Conference on Emerging Technologies: *Micro to Nano*; 2015 (ETMN-2015). DOI: 10.1063/1.4945168.

Pritha, C., Papiya, D., Sudeshna, C., Bohniskilda, C., Jayantihi, A. (2015). Cytotoxicity and antimicrobial activity of Colocasea esculenta. *Journal of Chemical and Pharmaceutical Research*. 2015;7(12):627-635.

Priyatharesini, P.I., Ganesamoorthy, R., Sudha, R. (2020). Synthesis of zinc oxide nanoparticle using *Cocos nucifera* male flower extract and analysis of their antimicrobial Activity. *J of Pharm and Tech*. 2020;13:2151- 2154.

Rad, S.S., Sani, A.M., Mohseni, S. (2019). Biosynthesis, characterization and antimicrobial activities of zinc oxide nanoparticles from leaf extract of *Mentha pulegium* (L.). *Microbial Pathogenesis*. 2019;131(2019):239–245.

Rahayu, V., Wonoputri, V., Nad Samadhi, T.W. (2011). Plant extract-assisted biosynthesis of zinc oxide nanoparticles and their antibacterial applications. *Material Science and Engineering*. 2020;823;012-036.

Rajiv, P., Rajeshwari, S., Venckatesh, R.. Rambutan. (2013). Peels promoted biomimetic synthesis of bioinspired zinc oxide nanochains for biomedical applications. Spectrochim. *Acta Part A Mol.Biomol.Spectros*. 2013;112:384–387. Available:http://dx.doi.org/10.1016/*j.saa*.2014.08.022.

Ramesh, P., Rajendran, A., Meenakshisundaram, M. (2014). Green synthesis of zinc oxide nanoparticles using flower extract Cassia auriculata. *J NS NT*. 2014;1(1):41–45. ISSN 2279 –0381.

Salam, A.H, Sivaraj, R., Venckatesh, R. (2014). Green synthesis and characterization of zinc oxide nanoparticles from *Ocimum basilicum*, L. *var. purpurascens, Benth.-Lamiaceae* leaf extract. *Mater.Lett*. 2014;131:16–18. Available:http://dx.doi.org/10.1016/j.matlet.2014.05.033.

Sadeghi, A., et al. (2019). "Antimicrobial effects of nanoparticles: A review." *Journal of Microbial and Biochemical Technology*. 10 (12): 12 -20.

Sangeetha, G., Rajeshwari, S., Venckatesh, R. (2011). Green synthesis of zinc oxide nanoparticles by *aloe barbadensis* miller leaf extract: Structure and optical properties. *Mater. Res. Bull*. 2011;46:2560–2566.

Sathishkumar, G., Rajkuberan, C., Manikandan, K., Prabukumar, S., DanielJohn, J., Sivaramakrishnan, S. (2017). Facile biosynthesis of antimicrobial zinc oxide (ZnO) Nano flakes using leaf extract of Couroupitaguianensis.Aubl, *Mater. Lett*. 2017;188:383–386.

Shiriki, D., Ubwa, S.T., Yusufu, M.I., Shambe, T. (2019). Extraction methods and inhibition studies of ten plant extracts on nine yam rot pathogenic microorganisms. *Food and Nutrition Sciences*; 2019. Available:https://doi.org10.4236/fns.2019.

Shiriki, D., Obochi, G.O., Eke, M.O, Shambe T. (2017). Postharvest Loss Control: Synergistic Plants Extract Inhibition of Ten Microbial Yam Rot Organisms. *Journal of food science and nutrition.*2017;8(7):25-732.

`

Sibiya, P.N, Moloto, M.J. (2014). Effect of precursor concentration and pH on the shape and size of starch capped silver selenide (Ag2Se) nanoparticles. Chalcogenide Letters. 2014;11(11):577-88.

Terngu, P.U., Anhwange, A., Okibe, F.G and Dooshima, S. (2024). *Green synthesis of Zinc Oxide Naniparticles using Colocasia esculenta* Tuber Peel Extract and Antimicrobial Studies Aganist White Yam Pathigens. *Asian J. Food Res. & Nutri., vol. 3, no. 2, pp. 306-319, 2024; Article no.AJFRN.116492.*

Terngu, P.U., Anhwange, A., Okibe, F.G and Dooshima, S. (2024). Isolation and Identification of Pathogens Associated with Posthharvest White Yam (Dioscorea rotundata L) *Tuber Rot. Asian J. Food Res. & Nutri.,* 3(3): 689-701.

Vijayakumar, S., Vinoj, G., Malaikozhunddan, B., Shanthi, S., Vaseeharan, B. (2015). Plectranthus amboinicus leaf extract mediated synthesis of zinc oxide nanoparticles and its control of methacillin resistant *Staphylococus aureus* biofilm and blood sucking mosquito larva. *Spectrochim. Acta Part Amol. Biomol. Spectrose*. 2015; 137:886-891. Available:http://dx.doi.org/10.1016/j.saa.2014.08.064.

Wang, J.K. (2019). Taro-a review of *Colocasia esculenta* and its potentials. *Journal of Biotechnology and Pharmaceutical Research*. 2012;3:42-46.

Yasser, S., Nassim, S. (2019). Current advances in applications of chitosan based nanaometal oxides as food preservative materials. *Nanomed J*. 2019;4:122-129.

Zare, E., Pourseyedi, S., Khatami, M., Darezereshki, E. (2017). Simple biosynthesis of zinc oxide nanoparticles using nature's source, and it's in vitro bio-activity. *Journal of Molecular Structure*. 2017;1146:96-103.

Zhang et al. (2018). Zinc oxide nanoparticles: A review of their synthesis, properties, and applications. *Journal of Nanomaterials*, 22(12): 1-13